Available online at www.sciencedirect.com
ScienceDirect
PERGAMON
Acta Astronautica 60 (2007) 166–174
ACTA ASTRONAUTICA
www.elsevier.com/locate/actaastro

Degradation of the surfaces exposed to the space environment

G. Bitetti[a,*], M. Marchetti[a], S. Mileti[a], F. Valente[a], S. Scaglione[b]

[a]*Department of Aerospace and Astronautical Engineering (DIAA), University "La Sapienza" Rome, Italy*
[b]*ENEA, CR Casaccia Rome, Italy*

Received 30 May 2005; accepted 18 July 2006

Abstract

The presence of several atomic species in the LEO (Low Earth Orbits) could be considered one of the reasons for the degradation of the surfaces exposed to the Space Environment.

At an average height of 400 Km (the altitude of International Space Station), the concentration of the main atomic species during the high sun activity are: $1.5 \times 10^9\,cm^{-3}$ for atomic oxygen (AO), $1.6 \times 10^8\,cm^{-3}$ for molecular nitrogen (N_2) and $1.4 \times 10^8\,m^{-3}$ for atomic nitrogen (N). The energy with which the atoms collide with the surface of orbiting vehicle depends on the relative speed of the vehicle itself. For instance, the atoms colliding the International Space Station (ISS) (orbit average height: 400 Km; relative speed: 7.5 Km/s) have an energy of 8 eV for N_2, 5 eV for OA and 4 eV for N.

The atomic oxygen is the most abundant species presents in LEO and it is considered the main responsible of the thermal, optical and mechanical alteration of the surfaces exposed to the Space Environment.

Different hypothesis are reported in literature in order to explain the physical/chemical mechanisms that govern the material degradation in the Space, but no conclusion has been reached.

In the energy range of few of eV, the main mechanism with which colliding atoms transfer its energy to the atoms of the surface is by phonons. In this paper the effect of an oxygen ion beam produced in the space environment simulator on materials for Space applications is studied in the frame of the thermal spike theory. Comparison between the measured erosion and the calculated one will be reported. The erosion mechanism will be modelled in order to understand the main thermodynamic parameters that govern the interaction between the atomic oxygen and the surface of the tested materials.

1. Introduction

The presence of several atomic species in the LEO orbits (Low Earth Orbits) could be considered one of the reasons for the degradation of the surfaces exposed to the Space Environment [1].

At an altitude between 200 and 700 km—a region where the Space Shuttle, the International Space Station and many other satellites orbit—the neutral atmosphere consists of O_2, N_2, Ar, He, H and atomic oxygen (AO) [2], which is a predominant constituent ($\sim$ 80%). The AO is produced by the photodissociation of molecular oxygen under Sun's short wavelenght UV radiation (100–200 nm range) and its density varies in relation to solar activity cycle, geomagnetism intensity, orbital altitude, orbital inclination, time of day, season etc.

At LEO altitudes, the number density of AO is almost 10^8 atoms/cm^3 for medium solar activity.

AO flux at International Space Station altitudes is approximately 1.0×10^{14} atoms/cm^2 s for normal incident ram surfaces.

* Corresponding author.
E-mail addresses: Grazia.Bitetti@uniroma1.it (G. Bitetti), mario.marchetti@uniroma1.it (M. Marchetti), sandromileti@libero.it (S. Mileti), faustavalente@libero.it (F. Valente), salvatore.scaglione@enea.casaccia.it (S. Scaglione).

0094-5765/$ - see front matter © 2006 Elsevier Ltd. All rights reserved.
doi:10.1016/j.actaastro.2006.07.019

In effect, although AO is the predominant species in LEO, these atoms have a very high probability of long-term survival in these altitudes because the mean free paths are on the order of 10^4 m at 400 km [3], giving an extremely low probability of oxygen atoms to recombine.

The average thermal velocity of the gas molecules at LEO altitudes is $\sim$ 0.4 km/s and the collision energy produced by their impact with spacecraft surfaces is too low to start any surface reaction.

However, when front surfaces (ram direction) of spacecrafts is orbiting in LEO at a velocity of about 7–8 km/s, the impacting kinetic energy between the spacecraft surfaces and oxygen atoms is approximatively 4.5–5 eV [4,2]. This energy value is high enough to break chemical bonds of most of the materials commonly used in space applications. The AO space vehicles' collision with this energy produces numerous chemical and physical events on the spacecraft surfaces [5].

Exposure of polymers and composite materials to the AO produces severe degradation effects that manifest themselves as materials mass loss and changes in their chemical, electrical, thermal-optical (sun light reflectivity and heat emissivity) and mechanical properties as well as surface erosion [1,5,6].

Polymeric films, such as Kapton, Mylar and polyuretane undergo drastic degradation by AO in LEO [7–9]. Polymers films are, in effect, widely used in space vehicles and systems as thermal blankets, sunshield and electrical control. To prevent and reduce the AO erosion, detailed studies on protective coatings for polymeric materials, including ceramic oxides, thin metallic film and siloxane coatings have been previously published [10].

In the present work, the results obtained by the AO erosion of polyimide samples in a plasma-type ground-based simulation facility are reported.

The materials chosen are Kapton HN and Kapton-ge films.

The Kapton is very often used in space applications for its thermal and electrical properties. It is also one of the main material used in space exposure and ground simulation research. It can be severely eroded by AO in LEO orbits.

The Kapton-ge is a germanium coated Kapton film, commonly used on the outer layer of MLI blanket to protect RF/microwave antennae from solar radiation. It is also used in LEO as protection from AO attack.

The AO effects on both were compared.

The erosion mechanism between oxygen ions and polymer film were tentatively hypothesized in terms of thermal spike and collision processes.

2. Experimental

The AO simulation tests were done using a ion source installed in the SAS, a Space Environment simulator, which belongs to "La Sapienza" University of Rome and located at the SASLab, a Laboratory of Aerospace and Astronautical Engineering Department.

2.1. The SAS simulator

The SAS simulator is constituted by a vacuum chamber, whose pump system is represented by a rotative pump and a Roots pump; a diffusion pump will be shortly installed on the SAS in order to obtain high vacuum chamber. The total clear volume inside the Simulator is about 5 m^3; the maximum vacuum level achievable is about 1.5×10^{-1} Pa.

The SAS is equipped with a thermal-vacuum cavity, whose dimensions are 1.5 m × 1 m × 1 m. The solar irradiance is simulated by means of IR quartz tubes, which total power irradiated amount is 1000 W/m^2; next to total emission of the Sun. The UV effects are simulated by UV lamps emission between 150 and 200 nm. The total power irradiated by UV lamps is 200 W/m^2. The SAS simulator is also equipped with a ion source for the simulation of AO effects on aerospace materials.

The SAS simulator is shown in Fig. 1.

2.2. The ground-based AO effects simulation facility (SCIS)

In order to simulate AO effects on the aerospace materials a single-cell ion source is installed on the SAS. The Source, shown in Fig. 2, is a cold cathode ion source produced by Advanced Energy Industries (USA).

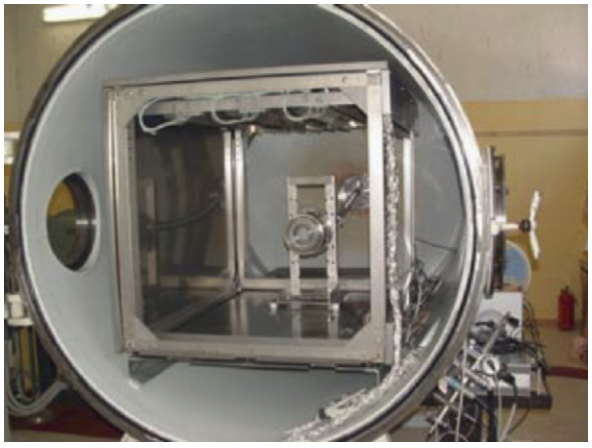

Fig. 1. SAS.

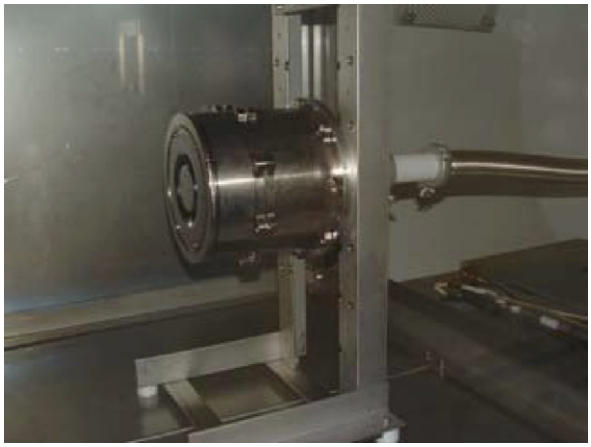

Fig. 2. Single-cell ion source.

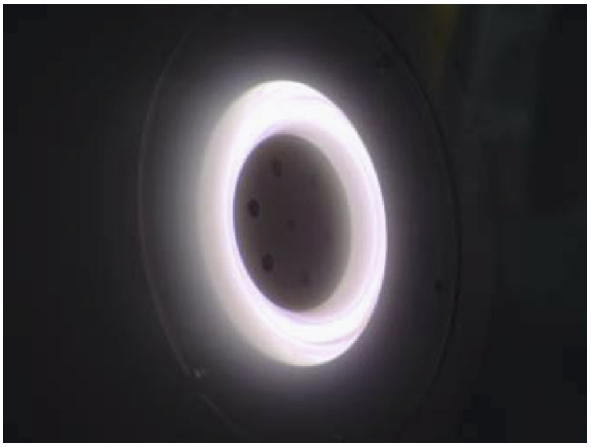

Fig. 3. Oxygen ion beam emitted by SCIS.

The SCIS basically constitutes of one anode and one cathode, magnetized by a permanent magnet.

The working gas (oxygen) coming from the external feeding system flows to the ion source through a separate feed-through and a flexible gas line and is controlled by a flow controller to reach a certain working pressure. Then a power supply delivers high voltage to the anode in the SCIS. An electric field is created between anode and cathode and the vacuum electrons are accelerated through it.

Since the cathode material is a soft steel, when it is magnetized by a permanent magnet, a magnetic field is created around the cathode and in front of the anode. A magnetic gap between external and internal cathode forms a circular emission slit.

Electrons, confined by magnetic field, collide with the gas and ionize it. The positively biased anode repels ions in the discharge area, and the ions accelerate away from the Source, creating the ion beam (visible in Fig. 3). On the contrary, the secondary electrons are attracted by the anode and come back to the source. In the ion source there is no hot filament, and it can operate for a long time without maintenance.

Most of the oxygen ions produced in the SCIS are single charged. As soon as an atom loses an electron, the electric field rapidly removes the ion from the discharge plasma before another collision with another electron can further ionize it.

2.3. Ion current beam measurement

To estimate the effects on the materials, the ion beam flux was measured by a Faraday cup manufactured by Kimball physics (model FC-72A). It consists of a

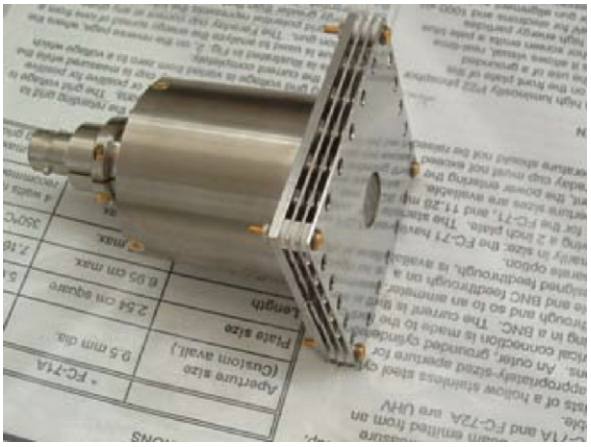

Fig. 4. The Faraday cup FC-72A.

hollow stainless steel cylinder closed at the base with an 1 cm^2 hole for collecting the ions (Fig. 4). An outer grounded cylinder provides shielding. An electrical connection is made to the base of the Faraday cup. The current is then conducted to a vacuum feed through and so to an ammeter. Once the ion current has been measured, the ion flux density (F) can be calculated:

$$F = I/(eA),$$

where e is the electronic charge; A the surface area of the collector; I the ion current.

The Faraday cup is equipped with a suppression grid, to reduce scattering of electrons or ions collected and to reduce secondary electrons emission. It is also equipped with a retarding grid to analyze the energy of ions collected.

Table 1
Working parameters

Experimental parameters	Value
Working pressure (Pa)	1.5×10^{-1}
Working temperature (°C)	25
Oxygen ion flux (ions/cm^2 s)	1.2×10^{15}
Total fluence (ions/cm^2)	4.3×10^{18}
O^+ energy (eV) 20% ion charge	267
O^+ energy (eV) 80% ion charge (O_2^+ split)	134

The ion beam flux carried out from the Faraday cup on the SAS AO simulation is 6.5×10^{14} ions/cm^2 s, but in order to calculate the oxygen ion flux, it is necessary to consider that during the functioning of the SCIS the oxygen ion beam is composed of almost 80% O_2^+ and 20% O^+ ions.

When the O_2^+ molecule impinges on the material surface, it splits producing two oxygen atoms, each having half of the initial O_2^+ energy. The flux related to O_2^+ ions is the sum of the flux of each oxygen atom produced.

Therefore, in order to calculate the effective oxygen ion flux that reaches the polymeric film surface, it is necessary to take in account the relative percentages of O^+ the O_2^+ in the beam. The effective oxygen ion flux is then 1.2×10^{15} ions/cm^2 s.

2.4. Working parameters

To investigate the reaction features of Kapton HN and Kapton-germanium in the SAS ground-based simulation facility, the samples were directly exposed to the oxygen ion beam formed by the discharge. The particles impinging on the samples include O_2, O, O^+, O_2^+ and electrons.

Two samples with size of 5×5 cm were derived from 50 μm thick sheets of Polyimide Kapton HN (DuPont) and Kapton-germanium. In general, germanium coating thickness may be varied according to the thermal properties of the blanket, but nominal germanium thickness is 1500 Å.

Before oxygen ion beam exposure, the samples were dehydrated 24 h in vacuum to favour the materials out gassing.

The samples are exposed for 1 h at oxygen ion beam at a distance of 5 cm from ion source emission slit.

Table 1 Lists the AO exposure parameters.

In Fig. 5, a Kapton HN sample during oxygen plasma exposure is shown.

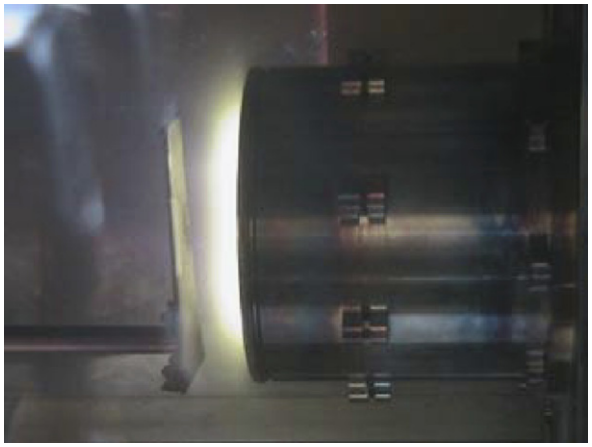

Fig. 5. Kapton HN sample during ion beam exposure.

2.5. Analysis methods

It is known that the Kapton mass increases due to the water absorption while it is exposed in air and decreases because of the dehydration in the vacuum chamber. Then, usually, Kapton HN have to be fully dehydrated in vacuum and immediately weighed prior and after exposure in order to minimize errors in mass due to the moisture absorption process.

Profilometer measurement technique was used to avoid this problem. This, actually, permits to evaluate the variation of film thickness, once it has been exposed to the ion beam, without taking into account moisture influence. In order to measure the amount of the eroded material, the samples were masked and the step was measured by a profilometer manufactured by TENCOR (model P10).

A field emission Scanning Electron Microscopy (SEM) (LEO 1530) was used to evaluate the change in surface morphology of polymeric films exposed to ion oxygen beam.

The measurements were performed at ENEA Research Centre.

3. Results and discussion

The Kapton HN is a polymer, whose main chain is represented by a imide structure. The AO action on this material is manifested by the formation of volatile oxide (CO and CO_2), with the consequent mass loss of the sample and the surface erosion.

Before the experiment, the Kapton HN film was in aspect amber, transparent and glossy. It yellowed afterwards.

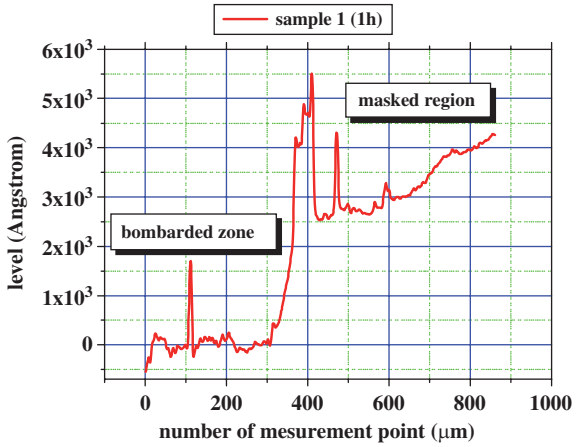

Fig. 6. Kapton HN sample optical profilometric result.

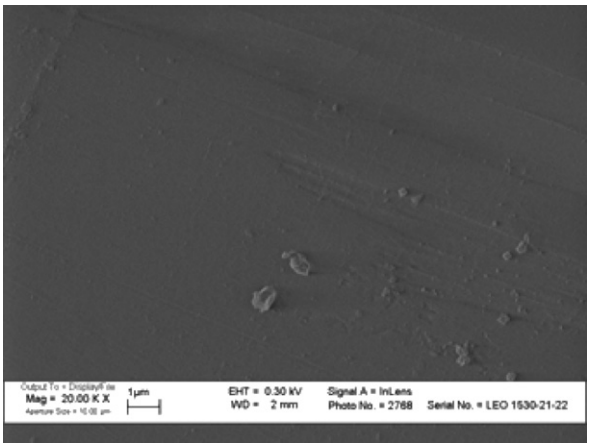

Fig. 7. SEM micrograph of Kapton HN sample before oxygen ion beam exposure.

The oxygen plasma in the SAS facility erodes Kapton significantly and results in considerable mass loss.

The results of profilometer measurements is displayed in Fig. 6. It is possible to notice a change in thickness between the exposed and the masked sample. The value of recession depth is about 0.3 μm.

Since Kapton HN density (ρ) equals to 1.42 g/cm^3, for 1 cm^2 surface (A) exposed to ion oxygen beam the 0.3 μm recession depth ($\Delta\delta$) equals to a mass loss of

$$\Delta m = \Delta V.\rho = A\Delta\delta.\rho = 4.26 \times 10^{-2}\ \text{mg}.$$

The surface morphology of the Kapton film changes significantly after the oxygen ion beam exposure.

The changes resulted from all the species present in the oxygen plasma environment of the SAS facility, including atoms, ions, molecules and electrons.

Fig. 7 shows a SEM micrograph of the Kapton HN sample before the oxygen ion exposure at magnification × 20 000. It shows that the sample surface is very smooth.

Fig. 8 shows a SEM micrograph of Kapton HN sample after 1 h oxygen ion beam exposure at magnification × 60 000; the fluence is 4.3 × 10^{18} ions/cm^2.

In this figure, the effect of the oxygen plasma is significantly appreciable: the surface of the sample appears eroded and it has a 'cone-like' or carpet-type morphology. This characteristic is typical of directed AO erosion on materials which produce gaseous oxidation.

This phenomenon reduces drastically ultraviolet-visible and infrared transmission.

The features of the surface are comparable with another picture obtained by NASA referred to AO exposure of a Kapton sample on board the LDEF facility [11].

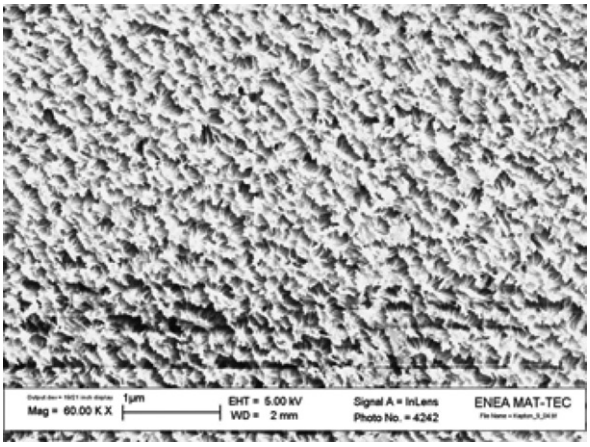

Fig. 8. SEM micrograph of Kapton HN sample after 1 h oxygen ion beam exposure.

Figs. 9 and 10 show a comparison between Kapton HN SEM images. Fig. 9 is a zoom of the micrograph shown in Fig. 8. Fig. 10 is the Kapton sample exposed on the LDEF.

It is possible to observe the similar 'cone-like' texture in both the pictures.

The comparison is also possible with other SEM results related to ground-simulate experiments previously published [2,12].

In the SEM of Fig. 8, the erosion morphology appears isotropic indicating that the impinging oxygen ions come from the normal direction.

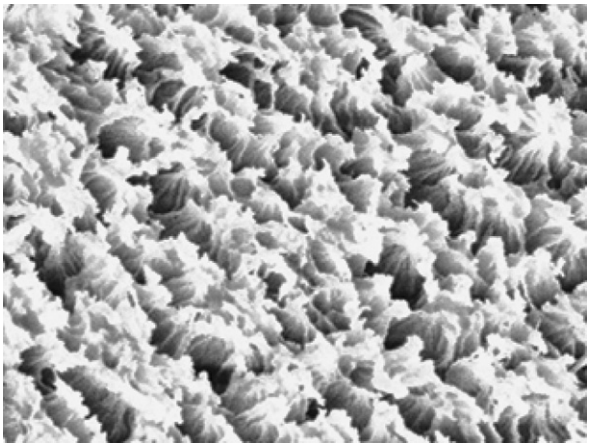

Fig. 9. Zoom of the SEM micrograph shown in Fig. 8.

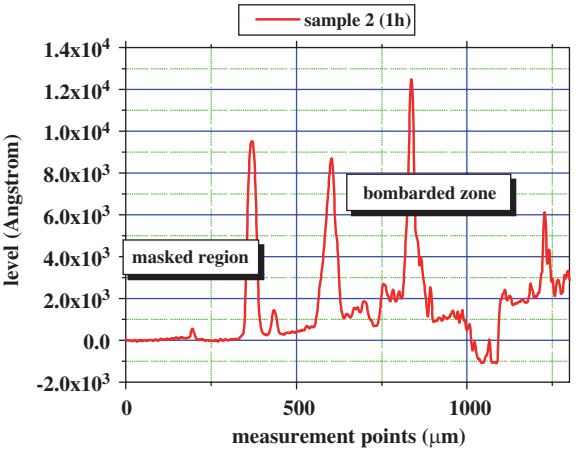

Fig. 11. Kapton-ge sample optical profilometric result.

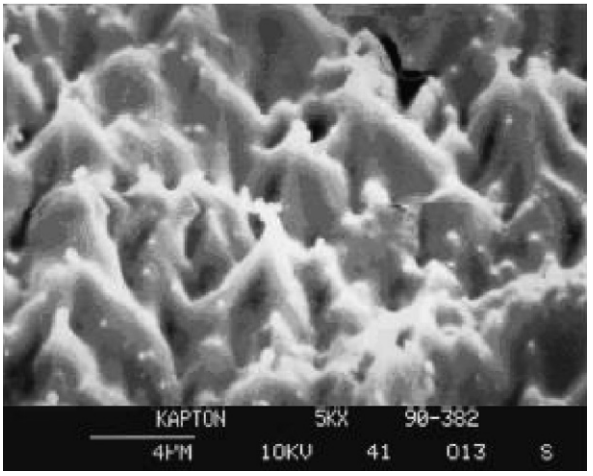

Fig. 10. SEM micrograph of Kapton sample exposed to OA on the LDEF facility.

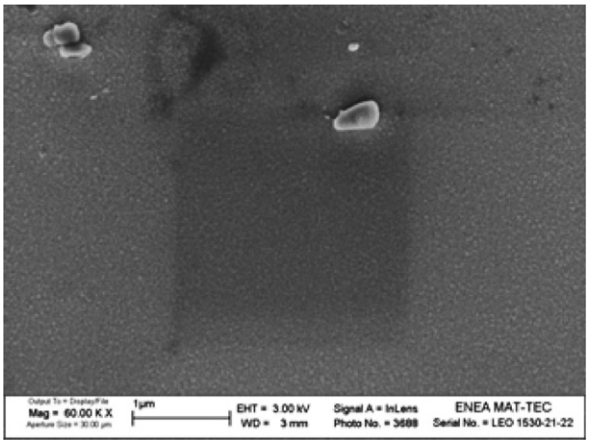

Fig. 12. SEM micrography of Kapton-ge sample before oxygen beam exposure.

This is a typical effect produced when the tests are carried out from on-ground facilities; the texture of the in situ exposed Kapton sample appears, infact, far more rough and oriented in the direction of oxygen atoms arrival [12].

Differently from the Kapton HN film, the erosion rate of germanium coated Kapton due to oxygen atoms exposure is considerably reduced compared to the erosion rate of unprotected Kapton [13].

However, the profilometric analysis gives no appreciable mass loss, but only an increasing roughness after AO exposure, as it is possible to observe in Fig. 11.

A possible explanation could be that, when impacted by oxygen ion, a stable oxide is formed on the surface of the germanium. This oxide layer can inhibit the diffusion of oxygen atoms within the film surface, preventing further degradation of the underneath surface. The germanium oxide acts like a protection for the Kapton HN film from AO erosion.

Since germanium develops durable oxide, the range of protection provided by this coating is a measure of the defect area of the coating.

Figs. 12 and 13 show, respectively, SEM micrographs of the Kapton-ge sample before and after the ion oxygen exposure at magnification × 60 000. The sample in Fig. 12 was exposed for 1 h at ion oxygen beam with a fluence of 4.3×10^{18} ions/cm^2, the same fluence used for the Kapton HN exposure. Comparing the two pictures of Figs. 12 and 13, the morphology of the surface of the unexposed germanium appears different from the surface exposed to the oxygen ions, even though no

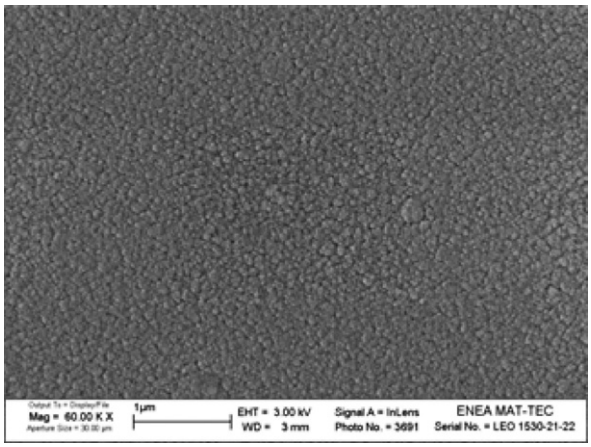

Fig. 13. SEM micrography of Kapton-ge sample after 1 h oxygen ion beam exposure.

appreciable mass loss was noticed, only a visible roughness of the surface. Probably, a mismatch between the structural parameters of the germanium and the germanium oxide is enough to cause a surface re-arrangement during the ion bombardment.

3.1. Erosion mechanism

The main drawbacks of using the ion source to produce oxygen for LEO environment simulation is that either the higher energy of the oxygen ions beam compared with the energy of the oxygen atoms present in LEO and also the possible different erosion mechanisms generated by neutral atoms instead of those generated by the ions. However, some consideration could be made in effects. In the last years, different hypothesis have been carried out about the interaction mechanism between low energy ions and materials. Due to these hypothesis, the damage related to atomic impact of various chemical species on surfaces in the Space Environment is considered due to either chemical processes (for the high reactivity of AO) or the physical processes. In the physical processes it is very important that the mechanism with which the starting energy of AO is transferred to the impacting surface.

Consider an atom that hits a surface, and after a number of impacts it comes to rest.

The possible mechanisms on how the atoms reach the stable condition are: interaction between electronic clouds, elastic impacts between nuclei and phononic emission, where phonon is a thermal energy (thermal spike) caused by the reticular wave vibration.

The starting energy value of the impacting atom determines the mechanism of how the energy is lost.

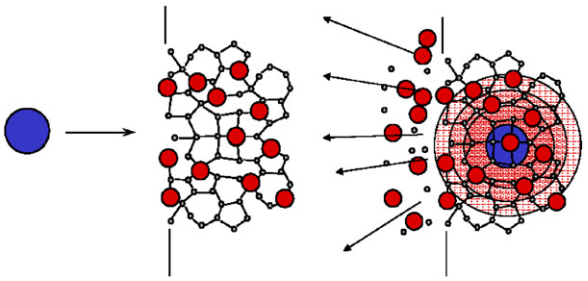

Fig. 14. Illustration of thermal spike process.

For high energy (higher than hundreds of KeV) the electronic interaction is more responsible in the process. For medium values of energy (between hundreds and tenths of eV) we have a major phenomenon of nuclei impacts up to lower energies where the phononic contribution becomes the only cause of the loss of energy.

Due the low impacting energy between the oxygen atoms and the surface in the Space Environment, the dominating mechanism is the thermal spike generation in the spot in which the atom impacts on the surface. At this point the local temperature increases significantly.

3.2. Thermal spike theory

Assuming the thermal diffusion coefficient constant, in the zone where the energy is converted to phonons the thermal energy dissipation follows the Fourier's law.

The solution of Fourier's equation which describes the course of the temperature related to the distance from thermal spike r and to time t is the following:

$$T(r,t) = \frac{E_{\mathrm{ph}}}{(8\pi^{3/2}c\rho)} \cdot \frac{1}{(D\cdot t)^{3/2}} \mathrm{e}^{-r^2/4D-t}, \qquad (1)$$

where E is the energy of the hitting atom; D the diffusion coefficient, co-related to the thermal conductivity, specific heat and to the material's surface density.

Calculating the temperature distribution with respect to the Spike distance for several values of time we can notice an area, a sphere in a three-dimensional vision, where the temperature reaches values over the sublimation value.

Therefore, we can believe that if the sphere has a $T > T_{\mathrm{sub}}$ and its radius reaches the impacted surface of the sample we have sublimation of the material on the surface which generates a crater.

The process is illustrated in Fig. 14.

From Eq. (2) it is possible to calculate t_{coll} which is the gap of time where the impacting atom of mass M

Table 2
Results of numerical simulation

Material	Energy (eV)	Yield		Phonon (% of ion energy)	
Kapton		Total		Ion	Recoils
	134	0.10		39.8	34.0
	60	0.03		60.0	19.7
	10	0		81.0	4.3
GeO_2		Y(Ge)	Y(O)		
	134	0.19	0.54	37.2	11.3
	60	0.08	0.23	57.3	21.3
	10	0	0	82.1	3.4

and energy E looses all it's energy:

$$t_{\text{coll}} = \frac{\sqrt{2 \cdot M_{\text{Oxygen}} \cdot E_{\text{Oxygen}}}}{\mathrm{d}E/\mathrm{d}x}. \quad (2)$$

Comparing t_{coll} with the time of the temperature dissipation, which vary for different types of material, it is possible to have estimation of the probability that this process may occur.

The thermal spike theory is performed by a Monte-Carlo based Code (SRIM 2003 by J.F. Ziegler and J.P. Biersack).

Simulating the impact of Kapton HN and the Kapton-ge by oxygen ions, the ion energy is released to the atoms of the surface by phonons and momentum transfer depending on the ion energy.

In Table 2 are reported the results of simulation.

The sputtering yield (Yield) is defined as the number of atoms that leave the surface per incident ion. As can be seen from Table 2, increasing the energy, the percentage of the ion energy released by phonons decreases, while the sputtering yield (collision process) increases as well. From Table 2, it could be inferred that at low energy the erosion effect is mainly generated by phonons processes (local thermal spike). Since the thermal spike processes depend on the thermal properties of the material (thermal diffusion coefficient), the AO erosion of metals and oxides is lower than that of the polymers.

For the Kapton HN sample, at the test energy value (134 eV), the collision time results $t_{\text{coll}} \approx 10^{-14}$ s.

In Fig. 15 is shown that at the t_{coll} the volume of the sphere of radius = 0.546 nm has $T > T_{\text{sub}}$, then the thermal spike process occurs.

The Kapton HN mass loss estimated by the spherical thermal spike model is

$$\Delta m_{\text{num}} = FT \cdot V_{\text{fus}} \cdot \rho_{\text{m}} = 4.79 \times 10^{-2}\,\text{mg}, \quad (3)$$

where FT is the total fluence; V_{fus} the Volume of the sphere heated at $T(r_{\text{fus}}, t_{\text{coll}}) > T_{\text{fus}}$; ρ_{m} the Kapton mass density (1.42 gr/cm^3).

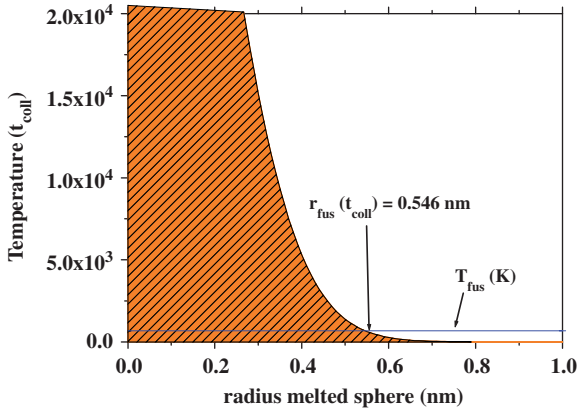

Fig. 15. Temperature distribution on the sphere centered on the thermal spike for Kapton HN sample.

4. Conclusions

The present work has emphasized the dangerous effects of the AO on space polymeric films commonly used for spacecraft thermal control in LEO.

After exposure to the oxygen ion beam produced by single-cell ion source, the Kapton HN sample appears yellow in aspect and it showed a significant mass loss, considering the low fluence of the exposure. On the SAS facility it is then possible to accelerate the aging experiments in comparison to in situ materials exposures.

After the oxygen ion exposure, the surface morphology of the Kapton HN sample is greatly changed: from SEM micrographs it is clear that the sample surface presents the typical "carpet-like" aspect, the same that polymeric thin films show after AO tests carried out on the other on-ground facilities.

The micrograph also shows the isotropic erosion morphology, indicating that the direction of the ions is normal to the surface of the sample.

However, the surface morphology of the Kapton HN sample exposed at AO in the SAS is comparable to the ones that were exposed to AO "in situ". The germanium coated Kapton shows, at the exposure conditions of the Kapton HN sample, only a surface roughness change, but no significant mass loss.

Probably, at high energy, the GeO_2 surface suffers of oxygen and germanium atom depletion during the Oxygen exposure; the impacting ion could substitute the oxygen loss, while the amount of lost germanium is very low (low sputtering yield).

The erosion mechanisms, simulated by MonteCarlo theory, were tentatively explained in terms of simultaneous thermal spike and collision process effects.

This method provides a physical approach to analyze the interaction process between oxygen and material surface. For all energy values reported in Table 2, as a consequence of low sputtering yield value, the thermal spike seems to be the main responsible for polymer degradation under oxygen ion exposure.

The numerical simulation carried out with the SRIM 2003 Code gives results very close to those obtained with the experimental tests.

References

[1] E. Grossman, I. Gouzman, Space environment effects on polymers in low earth orbit, Nuclear Instruments and Methods in Physics Research B 208 (2003) 48–57.
[2] X.-H. Zhao, Z.-G. Shen, Y.-S. Xing, S.-L. Ma, A study of the reaction characteristics and mechanism of kapton in a plasma-type ground-based atomic oxygen effects simulation facility, Journal of Physics D: Applied Physics 34 (2001).
[3] B.A. Banks, E.A. Sechkar, Space Flight Experiments to Measure Polymer Erosion and Contamination on Spacecraft NASA TM-211553, 2002.
[4] E. Grossman, Y. Lifshitz, J.T. Wolan, Ch.K. Moung, G.B. Hoflund, In situ erosion study of kapton using novel hyperthermal oxygen atom source, Journal of Spacecraft and Rockets 36 (1) (1999).
[5] T.K. Minton, D. Garton, Dynamics of atomic-oxygen-induced polymer degradation in low earth orbit, Chemical dynamics in estreme environments, Advanced Series in Physical Chemistry 11 (2001).
[6] D.A. Vance, M. McCargo, R. Hastert, M. Katz, J.P. Ochsner, Atomic oxygen-resistant polymer for use in the low earth orbit, IEEE 899593, 1989.
[7] Ph.R. Young, S.S. Wayne, The performance of selected polymeric materials exposed to low earth orbit, Polymers for Advanced Technologies 9 (1998) 20–33.
[8] M. Reddy Raja, Review effect of low earth orbit atomic oxygen on spacecraft materials, Journal of Materials Science 30 (1995).
[9] S.K. Rutledge, B.A. Banks, Atomic oxygen texturing of polymers and carbons, NASA TM-107521, 1997.
[10] S. Packirisamy, D. Schwam, M.H. Litt, Review atomic oxygen resistant coatings for low earth orbit space structures, Journal of Materials Science 30 (1995).
[11] D. Dooling, M.M. Finckenor, Material selection guidelines to limit atomic oxygen effects on spacecraft surfaces, NASA TP 209260, 1999.
[12] B.A. Banks, T.J. Stueber, S.A. Snyder, S.K. Rutledge, M.J. Norris, Atomic Oxygen Erosion Phenomena Defense and Space Programs, Conference Huntsville, Alabama, 1997.
[13] E.M. Silverman, Space environmental effects on spacecraft: LEO materials selection guide, NASA CR 4661, 1995.